文章编号：1005-5630(2011)01-0062-08

Study of real time eye location based on the retinal light reflection*

LAN Jingheng, GUO Hanming, ZHUANG Songlin
(School of Optical-Electrical and Computer Engineering, University of Shanghai for Science and Technology, Shanghai 200093, China)

Abstract: On the basis of the retinal light reflection, a method for real time eye location is proposed. Its feasibility is proved through the primary experiment of the judgment of the eye orientation. In this method, if there are no eyes in the cone-shaped illumination region of a point light source, no light spot also exists at the CCD and the image received by the CCD is an equably dark background. However, if there is an eye in the cone-shaped illumination region, the image captured by the CCD is a small bright light spot with dark background. The existent state, the orientation, and the location, relative to the point light source, of the eye can be derived from the position of the small bright light spot at the image captured by the CCD.

Key words: eye location; retinal light reflection; line of sight

基于视网膜光反射的实时人眼定位研究*

蓝景恒，郭汉明，庄松林
（上海理工大学 光电信息与计算机工程学院，上海 200093）

摘要：基于视网膜光反射，提出了一种只需要简单算法的实时人眼定位方法。通过确定人眼相对于点光源的空间方位的实验，证明了该人眼定位方法的可行性。在这种人眼定位方法中，如果在点光源形成的锥形照明区域中没有人眼，那么CCD接收的图像将是一个均匀的暗背景图像，且图像中没有亮斑存在；如果在该锥形照明区域中有人眼，那么CCD接收的图像将是一个具有均匀暗背景和存在微小亮斑的图形。根据该微小亮斑在CCD接收图像中的位置，可以判断人眼存在与否的状态，计算人眼相对于点光源的空间方位及位置。

关键词：人眼定位；视网膜光反射；视线
中图分类号：TM 930.12 **文献标识码**：A **doi**：10.3969/j.issn.1005-5630.2011.01.015

Introduction

Eye location is very useful for many vision-based applications, such as intelligent man-machine interfaces[1], face identification and recognition[2], driver behavior analysis[3,4], pathological analysis[5], and so on. The most widely practiced techniques detecting the eye location is to utilize various eye features[6]. The typical features that may be tracked mostly include the pupil[7-10] and reflection images formed by the cornea and the eye lens[9]. For

* 收稿日期：2010-08-09
基金项目：国家自然科学基金资助项目(60777045,60807007)；上海科技启明星基金资助项目(08QA14051)；上海市教育发展基金资助项目(2007CG61)
作者简介：蓝景恒(1985-)，男，广西都安县人，硕士研究生，主要从事光电检测方面的研究。

the pupil detection, the previous work[7-10] always use cameras to focus on the eye's pupil, so there are some complicated scene background, such as the hair, face, skin, brow, iris, white sclera, and so on, except for the pupil in the image detected by cameras. When the eye is illuminated along(or near to) the camera's viewing axis, the pupil appears bright in the image detected by cameras because of the eye's retroreflective properties. When the eye is illuminated off-axis the camera's viewing axis, the pupil appears dark in the image detected by cameras. Therefore, when a single light source is positioned on-axis or off-axis, it is usually required some complex algorithms, such as the thresholding images[9], a robust eye detection method[2], SVD transforms[7], and time-adaptive self-organizing map based active contour models[8], in order to eliminate the complicated scene background and locate the pupil. The other typical method is based on a differential lighting scheme using two light sources (on and off camera axis) to generate the bright/dark pupil images, which makes the scene background become irrelevant and the pupil be easily located. However, for the differential lighting technology using two light sources, due to fast motion of the head and/or eyes, the pupil is lost and detected again as soon as there is some pupil overlap between frames[9]. Moreover, if the motion is small, so that some overlap exists, pupils can still be detected, but motion artifacts might make this task more difficult[9].

While our detection technique is also based on the retinal light reflection, a special configuration of light source system is used. For example, the illumination light source is a point light source not but a extended light source(e. g. the ring light source used in Refs. 8-10) and the CCD without lens before itself is placed in a plane almost-but-not-quite conjugate with the retina. Therefore, in our detection technique, the image captured by the CCD is a bright light spot with dark background (i. e. no complicated scene background exists at the detected image) and the state, the orientation, and the location, relative to the point light source, of the eye are able to be calculated from the position of the bright light spot at the CCD with some simply algebraic formulas. Moreover, the detected accuracy is irrelevant of the motion of eyes. The detailed introduction and principle will be given later.

This paper is organized as follows. In Section 2, the principles for the determination of the existent state, the orientation, and the location, relative to the point light source, of the human eye based on the retinal light reflection are introduced in detail. Subsequently, a primary experiment of the judgment of the eye orientation is given in order to prove the validity of our detection technique in Section 3. Then, the method how to deal with the case that the eye does not gaze the point light source is discussed in detail in Section 4. Finally, some conclusions from this study are drawn.

1 Principle

As we know, an eye is an optical system in itself. Shown in Fig. 1, in the cone-shaped illumination region formed by the radiated lights of a point light source S_a, when the eye gazes the point light source S_a, the image due to the eye lens and the cornea of S_a is a very small light spot A at the retina and locates at the macula. At this time, the line AB, where the point B is the center of the pupil, represents the line of sight and the line S_aB is coincident with the line of sight. In addition, the small light spot A may be viewed a secondary source and its image due to the eye lens and the cornea is at the point S_a' because of the reflection of the retina, where the image point S_a' is the symmetrical point of S_a about the splitter of 45° if the thickness of the splitter is omitted.

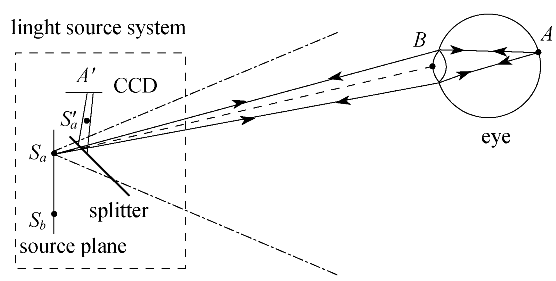

Fig. 1　Detection principle of the state of human eye based on the retinal light reflection

图 1　基于视网膜反射人眼定位的探测原理

Obviously, if a CCD is placed at the point S_a', there will be a small bright light spot (i. e. the image point S_a') at the image detected by the CCD. However, if there are no eyes in the cone-shaped illumination region, the above imaging process does not happen and no bright light spot exists at the image detected by the CCD. Moreover, as the reflected lights, arising from the scene background (i. e. the hair, face, skin, brow, iris, white sclera, and so on), detected by the CCD without lens before itself are very thin under the condition of the emanative illumination of the point light source, the image received by the CCD is an equably dark background. Therefore, the existent state of the small bright light spot at the image received by the CCD means whether there is an eye in the cone-shaped illumination region.

When the eye moves arbitrarily in the cone-shaped illumination region of S_a, the image point of the small light spot A always locates at the point S_a' if only the eye gazes the point light source S_a. Therefore, the point S_a' is a fixed point and only determined by S_a and the splitter. If a CCD is placed at the point S_a', the position of the small bright light spot A' detected by the CCD does not change with the movement of the eye and always is coincident with the point S_a'. However, if the CCD leaves a small distance of the point S_a' (see Fig. 1), the position of A' at the CCD will change with the movement of the eye. At this time, the orientation $S_a'A'$ corresponding to the point S_a' can be calculated from the position of A' at the CCD and the distance between the CCD and the point S_a', which will be given later. Actually, when the eye gazes the point light source S_a, the light rays will try back and converge into S_a if there is no splitter in Fig. 1. Here, the orientation S_aB, corresponding to the point light source S_a, of the eye will be equal to the orientation $S_a'A'$. Therefore, when one point light source (e. g. S_a) is adopted in Fig. 1, the orientation S_aB, corresponding to the point light source S_a, of the eye may be determined.

The above analyses always indicate that the eye should gaze the point light source, namely the orientation S_aB representing the line of sight. As the point light source in the line of sight might interfere with the visual task, one usually hopes that the eye does not gaze the point light source. If the point light source is far away from the line of sight, the bright light spot A' might be outside of the CCD, which makes it impossible to identify the orientation S_aB. However, if the point light source is not far away from the line of sight, the orientation S_aB can still be identified, which is proved by the later experiment.

Therefore, when the second point light source (e. g. S_b) is added in Fig. 1 and the distance between S_a and S_b is known and minor, the orientations S_bB and S_aB, separately corresponding to the point light sources S_b and S_a, of the eye may be also simultaneously obtained although the eye does not gaze the point light sources S_b and S_a. Here, the intersection point B of S_aB and S_bB is the position of the eye in 3D space. So the eye location relative to the two point light sources S_b and S_a can be calculated with a simple vectorial analysis when the distance between S_a and S_b and the orientations S_bB and S_aB are given.

2 Experiment

As indicated in Section 2, two point light sources are required for the determination of the eye location, but its basis principle is the same as that of the judgment of the eye orientation, where only one point light is needed. So, for the simplicity, a primary experiment of the judgment of the eye orientation will be given in this paper.

For the eye detection, the best light source is an infrared LED. Under ideal conditions (i. e. the eye gazing the point light source and the light source system being an ideal point source with high power), the size of the point S_a' is equal to that of the point light source S_a and is smaller than that of the bright light spot A' detected by CCD. In order to enhance the resolution of the orientation of the eye under the case of CCD with limited size, the size of S_a should be as small as possible. In addition, the power of the point light source S_a should be enough high, or the power of the bright light spot A' at the CCD will be too weak to be detected. Hence, the light source system shown in Fig. 1 should be designed carefully.

Without loss of generality, for the simplicity, the light source system in this paper is shown in Fig. 2. After the light emitted by a He-Ne laser is collimated and expanded, it is focused by a positive lens 1 with the focal length of 25.4mm into the pinhole 1 and forms the point light source S_a. The splitter is a cubic beamsplitter prism with side L of 24.5mm and the refractive index n of 1.51. The pinhole 2 with the diameter of 0.1mm locates at the point S_a' shown in Fig. 1 and its function is in order to eliminate the stray light spots because of the interference of lights arising from various surfaces (e.g. the surfaces of the beamsplitter prism and the pupil). If an infrared LED with high power is adopted, the pinhole 2 may be deleted because there is no interference. d denotes the distance between the CCD and the pinhole 2 (i.e. the point S_a'). The shape of the CCD is a rectangle with sides of 3.2mm×2.4mm and the eye is a simulated eye.

As shown in Fig. 2, the vertical dot dashed line through the pinhole 2 intersects with the CCD at its center. The origin o' of the coordinates $x'y'z'$ is also at the center of the CCD and the $x'y'$ plane represents the CCD plane. Assume the coordinates of the small bright light spot A' at the CCD (see Fig. 1) be (x', y'), the direction cosine angles corresponding to the x' and y' axes of the orientation $S_a'A'$ may be separately expressed as

$$\alpha = \mathrm{sign}(x')\arccos[x'^2/(x'^2 + y'^2 + d^2)]^{1/2}. \tag{1}$$

$$\beta = \mathrm{sign}(y')\arccos[y'^2/(x'^2 + y'^2 + d^2)]^{1/2}. \tag{2}$$

If the offset Δd due to the thickness of the beamsplitter prism is considered, in terms of Gaussian optics, the distance d between the CCD and the pinhole 2 in Eqs. (1-2) should be replaced with $(d-\Delta d)$, where $\Delta d = L(1-1/n) = 8.6$mm.

In the experiment, the simulated eye moves along the x axis in the xy plane with the distance of 685mm from the pinhole 1 plane (i.e. source plane shown in Fig. 1) and d is 19.5mm, where the horizontal dot dashed line through the pinhole 1 is the z axis of the coordinates xyz (see Fig. 2). During the course of the movement, the line of sight of the simulated eye is always along the z axis. In other words, only when the simulated eye arrives at the z axis, the eye gazes the point light source S_a, where as the eye does not gaze S_a for the other cases. In this experiment, the x coordinates of the simulated eye are EyePositions{27} = {−49.34, −46.08, −43.13, −34.69, −33.63, −34.33, −27.39, −26.41, −21.92, −15.19, −12.04, −12.44, −4.13, 0.56, 4.94, 9.06, 13.22, 17.18, 17.61, 21.16, 30.28, 30.62, 34.86, 38.26, 46.35, 48.47, 51.39} with the unit of mm, respectively. At this time, only the EyePosition[14] = 0.56 represents approximatively the case that eye gazes the point light source S_a. The small bright light spot A' detected by the CCD are shown in Fig. 3, which proves that, although the eye does not gaze the point light source, the orientation S_aB might still be identified.

Figure 3 is composed of 27 pictures corresponding to the above EyePositions. As the simulated eye only moves along the x axis, the individual picture is cut out along its center in the direction of the y axis. Shown in Fig. 3, there is always a fixed light spot in the center of the individual picture, which is due to the multi-reflections occurred in the upper and lower surfaces of the beamsplitter prism and is able to be eliminated by replacing the beamsplitter prism with a beamsplitting plate or the image processing. The other bright light spot in the individual picture denotes the bright light spot A' detected by the CCD, whose coordinates may be obtained by its relative position at the CCD multiplying the long side of the CCD, as follows: $x'[27]$ = {1.42, 1.24, 1.155, 1.038, 0.9536, 0.8901, 0.7947, 0.6464, 0.5616, 0.445, 0.3603, 0.3073, 0.1483, −0.0106, −0.2013, −0.2755, −0.3285, −0.3921, −0.5192, −0.6146, −0.7947, −0.8901, −1.007, −1.123, −1.229, −1.346, −1.494} with the unit of mm.

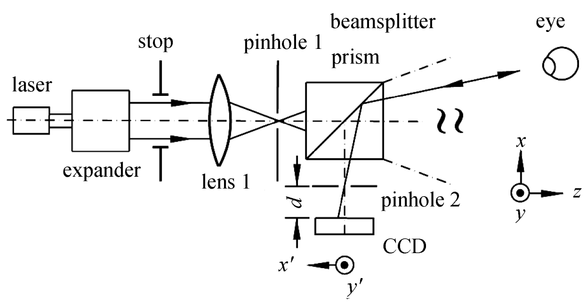

Fig. 2 Experimental schematic diagram of the judgment of the eye orientation

图2 判断人眼视线方向的实验原理图

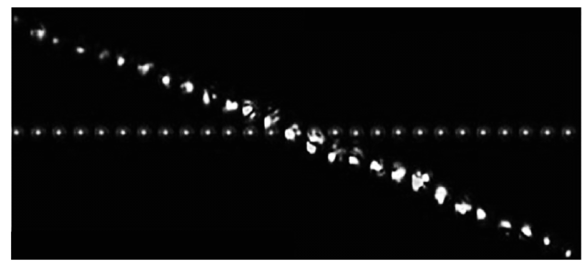

Fig. 3 The position of the image detected by a CCD with the movement of the eye

图3 随着眼睛的移动，CCD所探测到的图像的位置

In terms of Eqs. (1-2) with the offset Δd = 8.6mm considered, the direction cosine angles α of the orientation $S'_a A'$ with the movement of the simulated eye are shown in Tab. 1, where AV and MV denote actual values and measured values, respectively. It is inferred easily from Tab. 1 that the max absolute error is 0.35°. If the light source system shown in Fig. 1 is designed carefully and is integrated into a whole system instead of the isolated components as used in this paper, the lower errors can be obtained.

Tab. 1 The direction cosine angles α with the movement of the simulated eye, where *AV* and *MV* denote actual values and measured values, respectively

表1 随着仿真眼移动的方向余弦角 α，*AV* 是实际值，*MV* 是测量值

No.	*AV*(°)	*MV*(°)	No.	*AV*(°)	*MV*(°)	No.	*AV*(°)	*MV*(°)
1	−4.17	−4.14	10	−1.29	−1.30	19	1.49	1.52
2	−3.90	−3.62	11	−1.02	−1.05	20	1.79	1.80
3	−3.65	−3.37	12	−1.05	−0.90	21	2.56	2.32
4	−2.94	−3.03	13	−0.35	−0.43	22	2.59	2.60
5	−2.85	−2.79	14	0.05	0.03	23	2.95	2.94
6	−2.91	−2.60	15	0.42	0.59	24	3.24	3.28
7	−2.32	−2.32	16	0.77	0.81	25	3.92	3.59
8	−2.24	−1.89	17	1.12	0.96	26	4.10	3.93
9	−1.86	−1.64	18	1.45	1.15	27	4.34	4.36

3 Discussion

As introduced in Section 2, when the point light source is not far away from the line of sight (namely the eye also does not gaze the point light source), the size of the bright light spot A' detected by the CCD might still be enough small so that the orientation $S_a B$ may be identified. For example, for the experiment given in Section 3, the maximum distance between the point light source and the line of sight in the x axis is approximate ±50mm (see the 27th EyePositions) and the maximum range of the direction cosine angles α is approximate ±4.2° (see Tab. 1). When the distance between the point light source and the line of sight in the x axis is farther, the bright light spot A' will be outside of the CCD (see Fig. 3). In terms of Eqs. (1-2), the maximum range of the direction cosine angles is determined by the size of the

CCD and the distance d between the CCD and the point S'_a. Therefore, in order to increase the maximum detection range of the direction cosine angles d should be as small as possible under the case of meeting the given resolution of the direction cosine angles.

In addition, if the gazing point of the eye is far away from the point light source S_a in the z axis, the image A of S_a will be a large dispersion spot(i. e. S_1S_2) at the retina and the counterpart will be a larger dispersion spot(i. e. $S''_2S''_1$) at the CCD(see Fig. 4). Here, the size of the bright light spot A' detected by the CCD is enough large so as to cover the whole CCD, which makes that the state and position of the eye at the CCD cannot be identified. In order to deal with this problem, a lens 2 with the short focal length and the short depth of a field may be placed between the CCD and the reference plane(see Fig. 6), where the reference plane is the CCD plane of the Fig. 4. The function of the lens 2 is to focus the dispersion spot $S''_2S''_1$ at the reference plane into a smaller spot D_2 at the CCD. It is noted that the short depth of a field should be adopted for the lens 2. Only in this way can the complicated background not be detected by the CCD. In other words, if there are no eyes in the cone-shaped illumination region, the image received by the CCD still is an equably dark background although the lens 2 is placed before the CCD. Because of the smaller spot D_2 at the CCD, the lens 2 can not only enhance the resolution of the direction cosine angles α, but also increase the defocus distance $\Delta\varepsilon$, namely the distance between the gaze plane and the equivalent light source S'_a in the z axis(see Fig. 4).

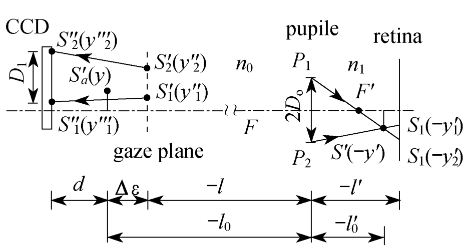

Fig. 4　Schematic diagram of optical path when the eye does not gaze the source plane

图 4　眼睛没有注视源平面时光路原理图

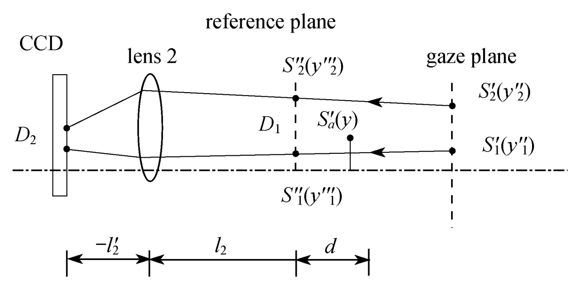

Fig. 5　Schematic diagram of optical path when a lens is placed between the CCD and the reference plane

图 5　物镜放置在 CCD 与参考平面之间的光路原理图

The rigorous imaging analysis of the lens 2 together with the eye lens and the cornea(see Fig. 4 and 5) is extremely difficult if the CCD plane is not parallel to the gaze plane. In order to make a preliminary estimation of the effect that the lens 2 placed between the CCD and the reference plane has, only a simple case is discussed, where the CCD plane is assumed parallel to the gaze plane (see Fig. 4 and 5) and Gaussian optics is used for the analysis method. Shown in Fig. 4 and 6, for the imaging relations due to the pupil(i. e the eye lens and the cornea) and the lens 2, the readers may infer from the object distance l_i and the corresponding image distance l'_i.

On the basis of Gaussian optics analysis of Fig. 4, it is easy to obtain the size D_1 of the light spot $S''_2S''_1$ at the reference plane, namely

$$D_1 = 2D_0\left|\frac{2(l_0-d)}{l}-\frac{(l_0-d)}{l_0}-1\right|+\Delta S \tag{3}$$

with its center height $y_{D1}=(-l_0+d)y/l_0$ at the reference plane, where l and l_0 represent the distance between the pupil and the gaze plane and the equivalent light source S'_a, respectively. D_0 denotes the radius of the pupil. ΔS is the size of the light source S_a. Then, the size of the light spot at the CCD is $D_2=MD_1$ with its center height $y_{D2}=My_{D1}$, where $M=l'_2/l_2$ is the magnify of the lens 2(see Fig. 5).

In the simulation calculation, let $d=3$mm, $l_2=40$mm, $l_2'=4$mm, $\Delta S=0.01$mm, $D_0=3$mm, and $l_0=685-\Delta d=676.4$mm, then the size D_2 of the light spot at the CCD is shown in Fig. 6. For the CCD with long side of 3.2mm, if the size $D_2=0.1$mm of the light spot at the CCD is assumed, the max defocus distances $\Delta\varepsilon$ are expanded -53.05mm and 59.35mm from -6.55mm and 3.6mm (see Fig. 6) when the lens 2 is used. Although the actual defocus distances $\Delta\varepsilon$ might be smaller when the rigorous imaging analysis is adopted, figure 7 also shows that the lens 2 may improve evidently the defocus distance $\Delta\varepsilon$.

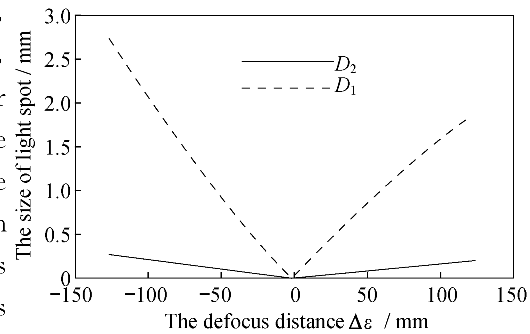

Fig. 6 The defocus distance $\Delta\varepsilon$ when the lens 2 is placed

图 6 放置物镜 2 的离焦距离 $\Delta\varepsilon$

4 Conclusion

The above experiment and analyses show that, on the basis of the retinal light reflection and the special configuration of light source system used in this paper, the eye orientation S_aB about the point light source S_a can be derived from the position of the small bright light spot A' at the CCD. If another point light source S_b is added and the distance S_aS_b is known (see Fig. 1), the eye location may be determined by the eye orientations S_aB and S_bB.

In addition, if there are no eyes in the cone-shaped illumination region formed by the point light source, no light spot also exists at the CCD and the image received by the CCD is an equably dark background. However, if there is an eye in the cone-shaped illumination region, the image captured by the CCD is a small bright light spot with dark background. Therefore, the appearance frequency of the light spot at the CCD can reflect the wink frequency of the eye, which can be used for the driver fatigue detection[11].

Finally, in theory, if the eye orientation S_aB is consist with the line of sight, the shape of the bright light spot A' at the CCD will be circular, or it will be elliptic. Moreover, as the image received by the CCD has equably dark background, it is possible to detect the shape of the bright light spot A'. Shown in Fig. 3, the shape of the bright light spot A' in picture 14 almost is the circularity, whereas it is not true for other pictures. The picture 14 of Fig. 3 corresponds to the 14th EyePosition=0.56 that represents approximatively the case of the eye orientation S_aB consisting with the line of sight. The major reason for the anomalous shape of the bright light spot A' except for the picture 14 is the interference because of laser used in Fig. 3. The other reason is that the pinhole 2 is not placed accurately. Hence, in terms the shape and orientation of the elliptic light spot at the CCD and the eye location, the line of sight might be determined if the noncoherent light source system is able to be designed carefully, which is very useful for the vision-based applications.

Reference:

[1] WANG P, JI Q. Multi-view face and eye detection using discriminant features[J]. *Comput Vision Image Understand*, 2007, 105: 99−111.

[2] SONG J, CHI Z, LIU J. A robust eye detection method using combined binary edge and intensity information[J]. *Pattern Recognition*, 2006, 39: 1110−1125.

[3] JIN S, PARK S Y, LEE J J. Driver fatigue detection using a genetic algorithm[J]. *Artif Life Robotics*, 2007, 11: 87−90.

[4] MARPLE-HORVAT D E, COOPER H L, GILBEY S L. Alcohol badly affects eye movements linked to steering, providing for automatic in-car detection of drink driving[J]. *Neuropsychopharmacology*, 2008, 33: 849−858.

[5] MITELMANA R, JOSHUAA M, ADLERA A, *et al*. A noninvasive, fast and inexpensive tool for the detection of eye open/closed

state in primates[J]. *J Neurosci Methods*, 2009, 178: 350－356.

[6] HUA H, KRISHNASWAMY P, ROLLAND J P. Video-based eyetracking methods and algorithms in head-mounted displays[J]. *Opt Express*, 2006, 14(10): 4328－4350.

[7] DANAFAR S, SHEIKH L T, TARGHI A T. A method for eye detection based on SVD transforms[J]. *Int J Imag Syst Tech*, 2007, 16: 222－229.

[8] KHOSRAVI M H, SAFABAKHSH R. Human eye sclera detection and tracking using a modified time-adaptive self-organizing map [J]. *Pattern Recognition*, 2008, 41: 2571－2593.

[9] MORIMOTO C H, KOONS D, AMIR A. Pupil detection and tracking using multiple light sources[J]. *Image Vision Comput*, 2000, 18: 331－335.

[10] JI Q, YANG X. Real-time eye, gaze, and face pose tracking for monitoring driver vigilance[J]. *Real-Time Imaging*, 2002, 8: 357－377.

消　息

活组织中分子运动实现“视频化”
新型 SRS 显微镜有助缩短外科手术时间

美国哈佛大学科学家将受激拉曼散射（SRS）显微镜和核磁共振成像（MRI）技术结合，研制出一种最新的生物医学成像设备，极大拓展了 SRS 显微镜的视野。其速度之快精度之高，如同“视频”，足以使科学家直接目睹分子在活组织中的运动。研究论文发表在最新一期《科学》杂志上。

“此前，SRS 显微镜每分钟只能拍摄一幅画面，用于活的动物或人体就太慢了。”哈佛大学化学与化学生物学教授谢晓亮说，“我们大大提高了采集数据的速度，使拍摄达到了视频速率。”研究小组还用这种新型 SRS 显微镜追踪药物在皮肤下的移动，其能清晰显示出药物实时吸收情况。如与内镜检查术结合，还能一层一层观察组织的三维结构。

新型 SRS 显微镜的工作原理是探测原子之间化学键的内在震动，由于融合了 MRI 技术，在透视深度上更适合拍摄体内器官和其他大目标，既可广泛用于拍摄器官和组织结构的静态图像，也能在亚细胞水平以流动画面观察细胞中的蛋白质、脂质和水。

同多种常用的观察生物分子的技术相比，新型 SRS 显微镜优势明显。它能采集分析照射生物样本的近 30％激光，比传统 SRS 显微镜高出 30 倍；并且不需要插入荧光标记，避免了绿色荧光标记蛋白质扰乱生物路径或压住较小生物分子的问题。此外，传统的红外显微镜空间分辨力太低，并需要给样本脱水；自然的拉曼显微镜需要很高的激光能量，整体耗时很长，在活样本中的应用受到限制；相干反斯托克拉曼散射显微镜在拍摄除了脂质以外的大多数分子时对比度不够，而新型 SRS 显微镜都能突破这些局限。

研究人员表示，新型 SRS 显微镜在医疗领域的应用前景广阔。比如，手术之前必须将样本送检以用于组织分析，这个过程大约要花 20min，其间病人需要等在手术台上，而新技术可提供实时扫描透视，有助于加速外科手术，清除肿瘤和其他损伤。谢晓亮说：“这一项目开始于 11 年前，核磁共振技术花了 30 多年才用于临床，我们期望这种 SRS 显微镜尽早应用于医院。”

（摘自《科技日报》）